Available online at www.sciencedirect.com
SCIENCE DIRECT®
Journal of Catalysis 231 (2005) 11–19
JOURNAL OF CATALYSIS
www.elsevier.com/locate/jcat

Structure sensitivity of ammonia synthesis over promoted ruthenium catalysts supported on graphitised carbon

Wioletta Raróg-Pilecka, Elżbieta Miśkiewicz, Dariusz Szmigiel, Zbigniew Kowalczyk *

Warsaw University of Technology, Faculty of Chemistry, Noakowskiego 3, 00-664 Warsaw, Poland

Received 5 October 2004; revised 2 December 2004; accepted 7 December 2004

Abstract

A series of carbon-based ruthenium catalysts differing in Ru loading (1–32 wt%) was characterised (XRD, TEM, O_2 and CO chemisorption) and, after promotion with Ba or Cs or both, was studied in NH_3 synthesis. Partly graphitised carbon with a high surface area ($S_{BET} = 1310\ m^2/g$) was used as a support for catalyst preparation. Ruthenium chloride and barium nitrate and/or caesium nitrate were precursors of the active phase and promoters, respectively. The chemisorption experiments have shown that the mean size of ruthenium particles (d) increases monotonically with Ru loading, from about 1 nm for 1 wt% Ru to about 4 nm for 32 wt% Ru. The NH_3 synthesis studies have revealed that the reaction rates (400 °C, 63 bar, 8.5% NH_3 or 400 °C, 90 bar, 11.5% NH_3), expressed in terms of TOF, increase versus particle size, regardless of the promoter type. Extrapolation to lower sizes indicates that crystallites smaller than 0.7–0.8 nm might be totally inactive. The co-promoted catalysts (Ba + Cs) were found to be more active than the singly doped systems over the whole range of the particle diameter. The trends in TOF versus d have been attributed to the promoter/promoters location, on the faces of the Ru crystallites, or, alternatively, to changes in crystallite morphology—larger particles (3–4 nm) may expose more B_5 sites than the smaller ones (1–2 nm). The effect of co-promotion has been ascribed to different modes of the promoters' action: whereas the main role of Cs is to lower the barrier for N_2 dissociation (electronic effect), barium acts predominantly as a structural promoter—the reconstructed surfaces in Ba–Ru/C are more resistant to poisoning by hydrogen when operating, thus making more sites available for N_2 adsorption.

Keywords: Ammonia synthesis; Ruthenium catalyst; Carbon support; Caesium and barium promoters; Ruthenium particle size effect

1. Introduction

The synthesis of ammonia from hydrogen and nitrogen is an important process in the chemical industry. Worldwide about 150 million tons of ammonia are manufactured annually, mainly in high-pressure installations operating with fused iron catalysts. The reaction $3H_2 + N_2 = 2NH_3$, proceeding on metal surfaces, is also important from the viewpoint of fundamental science [1]. New techniques in the field of heterogeneous catalysis and new catalytic concepts, including that of structure sensitivity, have been applied to this reaction [2].

The pioneering works on the structure sensitivity of ammonia synthesis reported experiments with systems based on iron. Dumesic et al. have shown in their fundamental papers [3,4] that the catalytic properties of small Fe particles deposited on magnesia (Fe/MgO) are essentially different from those of large particles. More specifically, the turnover frequencies (TOFs) of ammonia production over small crystallites (ca. 1.5 nm) were found to be an order of magnitude lower than those for large crystallites 30 nm in size. The difference was ascribed by the authors [3] to the presence of the so-called C-7 sites (iron atoms with seven nearest neighbours). As the concentration of C-7 atoms is expected to be smaller on very small Fe particles than on coarser ones, C-7 atoms were concluded to be more active than others in ammonia synthesis [3].

* Corresponding author.
E-mail address: zbyko@ch.pw.edu.pl (Z. Kowalczyk).

0021-9517/$ – see front matter
doi:10.1016/j.jcat.2004.12.005

To gain more insight into the nature of active Fe sites, the group of Somorjai determined NH_3 synthesis rates (400 °C, 20 bar, $H_2/N_2 = 3{:}1$) over single-crystal surfaces of well-defined geometry [5,6]. Such an approach made it possible to probe the effect of an iron structure directly. The Fe (111) and Fe (211) surfaces proved to be the most active planes, and they were followed in reactivity by Fe (100), Fe (210), and Fe (110) [5,6], the last of which was almost inactive. Since the Fe (111) and (211) faces are the only surfaces that expose C-7 sites to the reactant gases, the presence of C-7 sites was suggested [6] to be more important for an iron catalyst than surface roughness. Otherwise, the (210) plane, which exposes second- and third-layer atoms (open face), would be expected to be the most active plane [6].

In the last decade, carbon-based ruthenium catalysts were successfully introduced to industrial practice. High-capacity radial-flow reactors (2000 tons per day) operate under the Kellogg Brown & Root license, and they are filled with the conventional magnetite catalyst (first bed) and the ruthenium catalyst (three subsequent beds) [7,8]. Although the Ru-containing systems for NH_3 synthesis, including those supported on carbon, were studied extensively [9–49], only a few works have been devoted to the structure sensitivity of ruthenium. According to Dahl et al. [50], dissociative chemisorption of nitrogen (the rate-determining step of NH_3 synthesis) on the Ru (0001) single-crystal plane and N_2 desorption from Ru (0001) (the rate-limiting step of NH_3 decomposition) are totally dominated by steps; that is, the N_2 adsorption/desorption rates at steps are orders of magnitude higher than they are on/from the terraces. The above results, along with the DFT calculations, suggest [46,50] that ammonia synthesis over ruthenium should also be a very structure-sensitive reaction, even more so than on iron.

Jacobsen et al. [45] found that the activity of ruthenium deposited on a magnesium-aluminum spinel ($MgAl_2O_4$) increases slightly in the initial part of a NH_3 synthesis run; the effect is attributed to the disappearance of crystallites smaller than 1 nm due to sintering and the resulting formation of larger particles that expose higher reaction rates. In contrast, Szmigiel et al. have shown [51] the TOF of NH_3 synthesis over $Ru/MgAl_2O_4$ at 400 °C and 63 bar to be roughly independent of dispersion over the 0.9–1.5-nm particle size range. On the other hand, the same group has found [51] that extra fine (0.9 nm) Ru crystallites promoted with barium ($Ba–Ru/MgAl_2O_4$) exhibit an NH_3 synthesis rate expressed as TOF (63 bar, 400 °C, 8.5% NH_3) that is about half that exhibited by analogously promoted particles 1.5 nm in diameter.

As can be seen from these observations, the effect of particle size on the catalytic properties of ruthenium surfaces in NH_3 synthesis has been poorly documented so far. In particular, there is a lack of fully authoritative data for industrially relevant Ru/carbon systems; with this paper we attempt to fils this gap. The aim of our study was to show explicitly the relationship between the surface activity of ruthenium crystallites deposited on graphitised carbon and metal dispersion.

Generally, the Ru dispersion in Ru/C may be changed either by a change in the metal loading [20] or with the use of carbon materials of different textures [52]. The latter procedure may result, however, in different properties of the supports used. Furthermore, in the case of low-surface-area carbons, a broad profile of the particle size distribution is observed [17], which results in a poor estimation of the mean particle diameter. Therefore, the former option was chosen in this study; that is, ruthenium was deposited on the same carbon support of high surface area, and the metal loading was varied over a wide range of 1–32 wt%. Since unpromoted Ru/C catalysts are known to be almost inactive [17], kinetic studies of NH_3 synthesis were performed with promoted samples only. Both singly doped catalysts (Ba–Ru/C, Cs–Ru/C) and those co-promoted with barium and caesium (Ba–Cs–Ru/C) were tested. The dispersion of ruthenium was measured by the chemisorption technique; the sorption experiments were supplemented with XRD and TEM examinations. In contrast to activity measurements, the characterisation studies were carried out with unpromoted samples. It has been shown previously [47,53] that the Ru dispersion remains unchanged upon promotion when the catalysts are activated (reduced) under mild conditions, which is the present case.

2. Experimental

2.1. The catalysts

All of the ruthenium catalysts were deposited on a carbon support obtained via two-step modification of raw activated carbon supplied by the Research Centre of the Norit Company. Starting carbon (extrusions 2 mm in diameter) was heated under helium at 400 Pa pressure and 1900 °C for 2 h (first step) and then cooled to ambient temperature. Afterwards the carbon batch was gasified in a CO_2 stream at about 950 °C up to 35 wt% mass loss (second step). Finally, the material was washed with distilled water and dried in air at 120 °C.

For Ru/C, small samples of the carbon support were impregnated with acetone solutions of ruthenium chloride ($RuCl_3 \cdot 0.5H_2O$; Aldrich), followed by solvent evaporation in a rotary evaporator. After drying in air (90 °C, 24 h), the $RuCl_3$/C specimens were reduced in flowing hydrogen, first at 150 °C for 16 h and then at 350 °C for 24 h, followed by cooling to room temperature in argon and passivation with small pulses of air added to an Ar stream. In the case of high ruthenium contents (20 or 32 wt%), the impregnation–reduction–passivation procedure was repeated three and five times, respectively.

Barium nitrate or/and caesium nitrate, precursors of the promoters, were introduced to the Ru/C systems through impregnation from aqueous solutions at 90 °C for 16 h. Then

Table 1
Chemical composition of the promoted Ru/C catalysts

Catalyst symbol	Ru content in (Ru + C) (wt%)	Ba content ($mmol/g_C$)	Cs content ($mmol/g_C$)
Ba–Ru1/C	1	1.0	–
Ba–Ru3/C	3	1.0	–
Ba–Ru5/C	5	1.0	–
Ba–Ru9.1/C	9.1	1.0	–
Ba–Ru20/C	20	1.2	–
Ba–Ru32/C	32	1.3	–
Cs–Ru1/C	1	–	3.5
Cs–Ru3/C	3	–	3.3
Cs–Ru5/C	5	–	3.2
Cs–Ru9.1/C	9.1	–	3.3
Cs–Ru20/C	20	–	3.3
Cs–Ru32/C	32	–	3.6
Ba–Cs–Ru1/C	1	0.9	3.4
Ba–Cs–Ru3/C	3	0.8	3.2
Ba–Cs–Ru3/C(H_2)	3	0.8	3.3
Ba–Cs–Ru5/C	5	0.9	3.5
Ba–Cs–Ru9.1/C	9.1	0.9	3.4
Ba–Cs–Ru20/C	20	0.9	3.5
Ba–Cs–Ru32/C	32	1.0	3.8

the solid material was separated from the hot solution and dried in air at 110 °C for 16 h. The catalysts thus prepared were crushed and sieved to obtain 0.2–0.63-mm particles used subsequently in the NH_3 synthesis tests. The chemical characteristics of the catalysts are listed in Table 1. For clarity, the samples have been given uniform designations (e.g., Ba–Ru32/C) that specify the kind of the promoter and ruthenium loading (wt%) in the unpromoted materials (Ru + C). In one case (the sample labelled Ba–Cs–Ru3/C(H_2); see Table 1), carbon was additionally heated in hydrogen (700 °C, 20 h) before ruthenium deposition.

As seen in Table 1, the ratios of the promoter contents to the carbon mass were kept nearly constant: about 1 $mmol/g_C$ and about 3.5 $mmol/g_C$ for barium and caesium, respectively. Such values were found previously [20] to be optimal (maximum reaction rates versus the Ba or Cs contents) for similar Ru/C systems with different levels of Ru loading (the optimal promoter content, expressed in $g_{(Ba,Cs)}/g_C$, is independent of the active metal loading [20]).

2.2. Characterisation studies and activity measurements

The texture of the modified carbon support was characterised by nitrogen physisorption (Gemini 2360, Micromeritics) and mercury porosimetry (Auto Pore II 9215, Micromeritics). The Ru/C systems were characterised by chemisorption (O_2, CO) and XRD. Some TEM experiments were also performed.

The chemisorption studies were carried out in a fully automated Peak-4 instrument (manufactured by the Technical University of Łódź) equipped with a U-tube glass reactor and a thermal conductivity detector as an analytical tool. Before measurement, the samples were reduced in a hydrogen–helium (80:20) mixture of high purity (99.9999%, 40 ml/min) at 430 °C for 20 h, followed by cooling to 400 °C in a H_2–He stream, flushing with helium (99.9999%, 40 ml/min) at 400 °C for 0.5 h to remove hydrogen from the sample, and cooling in He. Then we determined the oxygen uptake at 0 °C by adding small O_2 pulses (6.25 μmol) to the helium stream. Afterwards, the procedure consisting of reduction (430 °C, 3 h) and flushing with He was repeated and the amount of carbon monoxide adsorbed on the metal surface at 20 °C was measured (pulse method). The uptakes of adsorbates were used for determining the dispersion of ruthenium (fraction exposed, FE) and the size of the metal particles (d). The latter parameter was calculated from the generalised formula proposed by Borodziński and Bonarowska [54]. The O:Ru_s (= 1:1) and CO:Ru_s (= 0.6:1) stoichiometries of adsorption were assumed [55,56] to recalculate the adsorbate uptake into the FE value.

The X-ray diffraction patterns were recorded with the standard Bragg–Brentano focusing geometry of a diffractometer (Siemens D5000) with CuK radiation (1.54A) filtered on nickel. We determined the average crystallite sizes of ruthenium from Scherrer's equation, using the integral widths of metal reflections fitted to the analytical Pearson VII functions. The TEM studies were performed with a Jeol JEM2000EX instrument equipped with a double tilted goniometer and operating at a 200-kV potential. The specimens were ground and dispersed in n-butanol. Drops of the suspensions were then placed on a holey carbon film supported by a copper grid.

The kinetic measurements of NH_3 synthesis were carried out in a differential reactor supplied with a high-purity (> 99.9999%) stoichiometric H_2–N_2–NH_3 mixture with a controlled ammonia concentration (x_1). A detailed description of the setup can be found elsewhere [57]. Under steady-state conditions of temperature (400 °C), gas flow rate (70 dm^3(STP)/h), pressure, and ammonia concentration in the inlet stream (63 bar, about 8% NH_3 or 90 bar, about 11% NH_3), small increments ($x_2 - x_1$) in the concentration of ammonia formed on the catalyst by the reaction were measured. Consequently, we could determine the NH_3 synthesis rate, corresponding to a mean value of $x = (x_1 + x_2)/2$ from a mass balance of the catalyst layer, assuming that the reactor operated as a plug-flow reactor [57]. Typically, small catalyst samples (50–150 mg) were used in the studies. Reduction (activation) of the samples was performed in a H_2:N_2 = 3:1 stream at 1 bar, according to the following temperature programme: heating to 400 °C and maintaining at 400 °C for 16 h, heating to 430 °C (Cs–Ru/C, Cs–Ba–Ru/C) or to 470 °C (Ba–Ru/C), and maintaining constant temperature for 24 and 48 h, respectively.

3. Results

3.1. Characterisation results

The textural parameters of the modified carbon support are collected in Table 2. For comparison, the data charac-

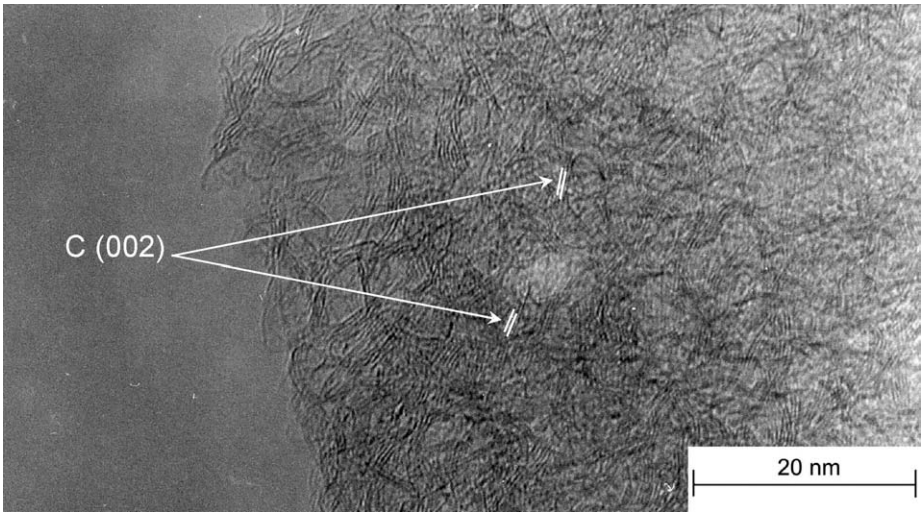

Fig. 1. HRTEM image of the carbon support; arrows indicate (002) lattice plane fringes.

Table 2
Textural parameters of carbons; S_{BET}—BET surface area; S_{Hg}, V_{Hg}—surface area and volume of pores determined by mercury porosimetry

Carbon material	S_{BET} (m^2/g)	S_{Hg} (m^2/g)	V_{Hg} (cm^3/g)
Raw carbon	1430	280	0.82
After 1900 °C	228	45	0.26
After gasification in CO_2	1310	267	0.77

terising starting carbon and those for the material heated at 1900 °C have also been included. It is clearly seen (Table 2) that the high-temperature treatment (first step) leads to a drastic decrease in the BET surface area (S_{BET}) and the area of pores accessible for mercury (S_{Hg}), in accord with the literature data obtained for various types of activated carbons [14,15,19,22,52,58]. However, the S_{BET} and S_{Hg} values corresponding to the resultant material (after subsequent gasification) are close to those of raw carbon, thus showing the gasification step to be very advantageous (a well-developed texture is essential for the preparation of highly dispersed Ru catalysts [52]). In contrast to raw carbon, the modified carbon is partly ordered (graphitised), as indicated by TEM (see Fig. 1), and is very pure (residue after ignition $< 0.05\%$).

Fig. 2 shows the XRD patterns of all of the unpromoted Ru/C specimens prepared. As expected, the contribution of Ru to the diffraction profiles depends strongly upon the Ru loading. The most intensive reflections correspond to the specimen with the highest ruthenium content (Ru32/C). The average crystallite size of about 3.5–4 nm results from the Ru (102) and (110) lines broadening for this material. Slightly weaker but still noticeable Ru reflections are seen in the Ru20/C pattern; the average crystallite size of 2.5–3 nm was estimated from the profile analysis. In the case of the other samples (Ru1/C, Ru3/C, Ru5/C, and Ru9.1/C), the XRD patterns are identical to that of the carbon support (see Fig. 2), thus indicating that the metal particles are very small in all

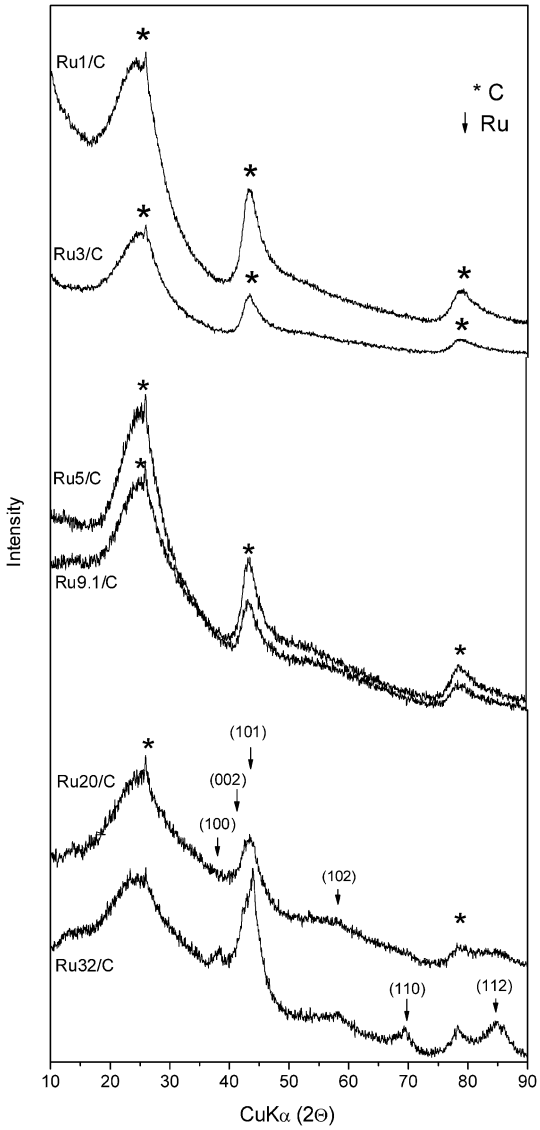

Fig. 2. XRD patterns of the Ru/C catalysts differing by the ruthenium loading.

Table 3
Chemisorptive characteristics of the unpromoted Ru/C catalysts

Catalyst	O_2 chemisorption		CO chemisorption	
	O_2 uptake ($\mu mol/g_{(C+Ru)}$)	FE_{O_2}[a]	CO uptake ($\mu mol/g_{(C+Ru)}$)	FE_{CO}[a]
Ru1/C	48.5	0.89	54.3	0.92
Ru3/C	142	0.87	159	0.89
Ru3/C(H_2)	140	0.86	154	0.87
Ru5/C	206	0.76	234	0.79
Ru9.1/C	332	0.67	376	0.695
Ru20/C	541	0.50	648	0.55
Ru32/C	496	0.285	608	0.32

[a] FE (fraction exposed) is defined as the number of surface Ru atoms referred to the total number of Ru atoms in the catalyst.

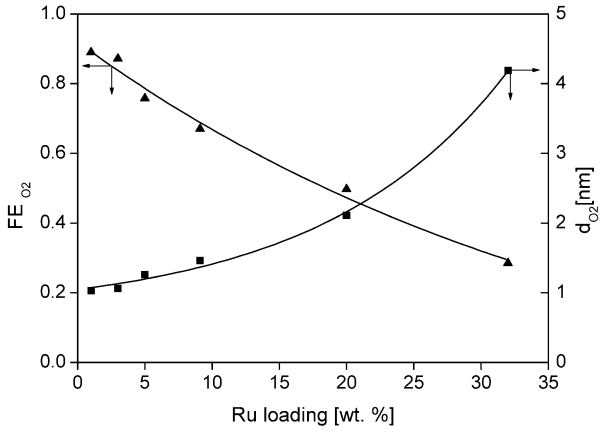

Fig. 3. Dispersion of ruthenium (FE_{O_2}, d_{O_2}) vs the metal loading in Ru/C.

of the specimens or, more precisely, that they are in a form that is not detectable with the conventional XRD technique.

The results of chemisorption studies performed with the Ru/C catalysts are collected in Table 3. Neither carbon monoxide nor oxygen was adsorbed on the carbon support, as indicated by the blank experiments. So the adsorbate "uptakes" listed in Table 3 can be ascribed solely to the presence of ruthenium in the materials. In general, there is good agreement between the chemisorption data obtained for oxygen and those for CO. The difference between FE_{O_2} and FE_{CO} does not exceed 15% and is usually significantly smaller. The dispersion expressed as FE decreases monotonically (Fig. 3), and, correspondingly, the average crystallite size increases (Fig. 3) vs metal loading, but the effect is rather weak. Whereas the Ru content varies by a factor of about 30, the average crystallite size varies by a factor of 4 only. It is worth noticing that the Ru1/C and Ru3/C samples have almost identical dispersions (crystallite size), in spite of a large difference in the metal loading.

Fig. 4 presents a high-resolution image (HRTEM) obtained for one of the Ru/C samples (Ru20/C). As seen, rather well-shaped ruthenium particles about 2 nm in diameter dominate the carbon support, in accord with the chemisorption results ($d_{O_2} = 2.1$ nm, $d_{CO} = 1.88$ nm). A narrow range of the crystallite sizes in the catalysts is of crucial importance when the average crystallite size determined from the chemisorption data is correlated with the surface-based reaction rates of ammonia production.

Table 4
Rates of ammonia synthesis over the promoted Ru/C catalysts

Catalyst precursor	Reaction rate ($gNH_3/g_{(C+Ru)}$ h)		
	Ba–Ru/C	Cs–Ru/C	Ba–Cs–Ru/C
(A) 400 °C, 63 bar, 8.5% NH_3			
Ru1/C	0.168	0.409	0.66
Ru3/C	0.654	1.60	2.18
Ru3/C(H_2)	–	–	2.2
Ru5/C	1.50	3.11	4.26
Ru9.1/C	3.47	5.96	8.20
Ru20/C	7.34	11.84	17.6
Ru32/C	8.62	11.2	18.6
(B) 400 °C, 90 bar, 11.5% NH_3			
Ru1/C	–	0.398	0.66
Ru3/C	0.726	1.63	2.08
Ru3/C(H_2)	–	–	2.10
Ru5/C	1.62	3.10	4.10
Ru9.1/C	3.78	5.94	7.74
Ru20/C	8.16	12.1	16.7
Ru32/C	9.48	12.4	18.2

3.2. Activity of the catalysts

The results of NH_3 synthesis studies are collected in Table 4. Part A of this table presents the data obtained under a lower pressure of 63 bar, and part B is related to a higher pressure of 90 bar. As one may notice, the NH_3 synthesis rates determined at 63 bar are close, correspondingly, to those determined at 90 bar ($r_i(63) = r_i(90)$); an advantageous effect of the pressure increase (90 vs 63) was counterbalanced totally by the enhancement in the ammonia concentration in the gas phase (11.5 vs 8.5%). The most relevant relationships (see below) resulting both from the NH_3 synthesis and chemisorption experiments will be based, therefore, on the kinetic data obtained under the low-pressure conditions (63 bar, 8.5% NH_3, 400 °C).

Fig. 5 illustrates the effect of the ruthenium particle size calculated from oxygen chemisorption (d_{O_2}) on the activity of differently promoted Ru/C catalysts; the reaction rates are related to the metal mass (r_{Ru}). It is clearly seen that the co-promoted catalysts (Ba + Cs) are more active than the singly promoted systems, in agreement with our previous results [20]. It is also seen that crystallites about 1.5–2.0 nm in diameter expose the highest reaction rates, regardless of the kind of promotion. The latter observation is important in practice. Ruthenium is an expensive metal, and its high productivity, related to its mass, is a key criterion of the catalyst's usefulness. It is a question of art or technology rather than of science, however, how to manufacture catalysts with optimal ruthenium dispersion and required loading. From a scientific point of view, the relationship between particle size and surface activity, expressed in terms of turnover frequencies, seems to be more essential. Such dependen-

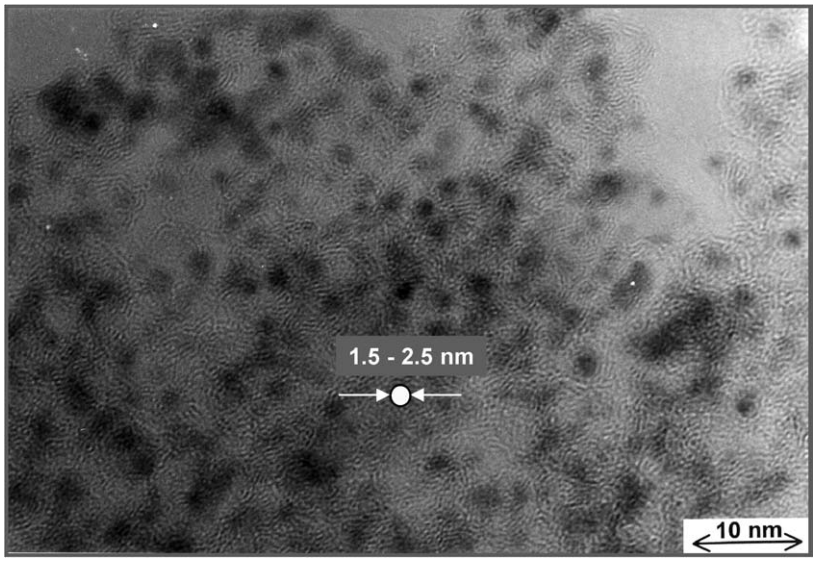

Fig. 4. HRTEM image of the Ru20/C system.

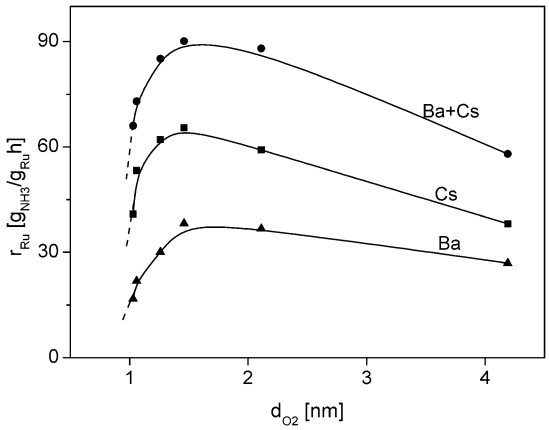

Fig. 5. Ammonia synthesis rate referred to the ruthenium mass (r_{Ru}) vs Ru particle size (d_{O_2}); $p = 63$ bar, $T = 400\,^{\circ}$C, 8.5% NH_3.

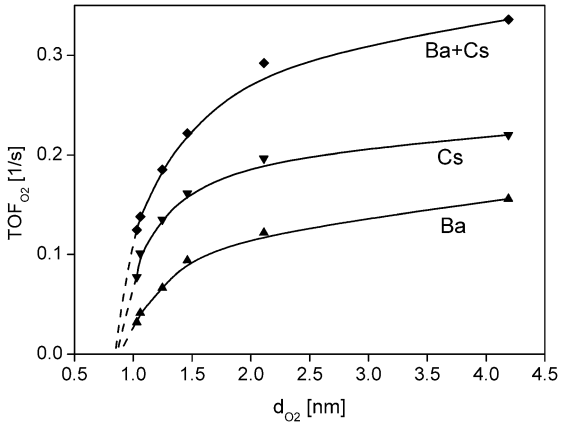

Fig. 6. Surface reaction rate (TOF_{O_2}) vs Ru particle size (d_{O_2}); $p = 63$ bar, $T = 400\,^{\circ}$C, 8.5% NH_3.

cies obtained for the three promoted systems are shown in Fig. 6; the TOF values are based on the kinetic and oxygen chemisorption data. A monotonic increase in TOF_{O_2} vs d_{O_2} is characteristic for each system. Extrapolation of the results to small crystallite diameters suggests (Fig. 6) that extra fine particles smaller than 0.7–0.8 nm (critical size) might be totally inactive. Analogous trends in the surface activities were found (not shown) when the amounts of adsorbed CO were used instead of O_2 uptake for the particle diameter and TOF calculation.

4. Discussion

We consider two possibilities when discussing the effect of the particle diameter (d) on the catalytic properties of ruthenium surfaces in ammonia synthesis (TOF): (1) interaction between ruthenium crystallites and the carbon substrate; and (2) the structure sensitivity of the NH_3 synthesis reaction, including the possibility of new active site formation by the promoters.

According to Zhong et al. [25,26] and Aika et al. [9], activated carbons interact with ruthenium (metal–support interaction). More specifically, some functional groups (oxygen complexes that are strongly bound to the carbon support) withdraw electrons from the ruthenium atoms, thus lowering the catalyst activity in ammonia synthesis (electron-poor surfaces are less active in nitrogen dissociative adsorption, which is believed to be the rate-limiting step of NH_3 synthesis). Since the interaction is in the local range, a disadvantageous effect of the oxygen-containing groups is expected to be weaker for larger particles, in accord with the trends of TOF presented in Fig. 6. Deactivation of ruthenium by oxygen complexes was observed recently by Raróg-Pilecka et al. [59] in the reaction of ammonia decomposition over unpromoted Ru/C systems: removal of oxygen complexes by preheating of the carbon support in a hydrogen stream at high temperature resulted in a drastic (about 6-fold) increase

in the NH_3 decomposition rate, although the Ru dispersion (73%) remained unchanged [59].

The above interpretation of the particle size effect on the TOF of NH_3 synthesis seems to be valid for the unpromoted Ru/C systems only. Recent in situ XPS and UPS studies performed by Muhler's group [60] and those of Shitova et al. [61] demonstrate that alkali (K, Cs in Ru/C) is strongly reduced under ammonia synthesis conditions (a substoichiometric alkali + O adlayer on both the graphitic support and the Ru particles [60], a partly metallic state of the alkali [61]). From a chemical point of view, the existence of oxygen complexes in the presence of the reduced promoter seems to be unlikely. Indeed, the Ba–Cs–Ru/C(H_2) sample derived from the carbon support preheated in hydrogen at 700 °C proved to be as active as that based on carbon that was not modified with H_2 (see Table 4); the dispersions of the materials compared were also identical (Table 3).

The structure sensitivity of ammonia synthesis on ruthenium is ascribed to the presence of the so-called B_5 sites, which are believed to be extremely active and thus to dominate the reaction rate [45]. The B_5-type sites may exist on the surfaces of various metals, such as platinum, palladium, nickel, or ruthenium, and they were early recognised to be responsible for strong physical adsorption of nitrogen [62]. According to Jacobsen et al. [45], a fraction of B_5 sites in the supported Ru catalysts depends on both the crystal morphology and its size; the morphology is determined by the kind of support material, as indicated by TEM studies of different systems—Ru/C, Ru/$MgAl_2O_4$, and Ru/Si_3N_4. Promoters, like barium, do not influence the number of active sites [47]. They modify electrostatically the potential around the B_5 sites (electronic promotion), making them significantly more active for N_2 dissociation [47]. Based on the statistics proposed by van Hardeveld and Hartog [63], the group of Jacobsen counted the relative number (in relation to the total number of atoms) of B_5 sites on hcp ruthenium crystallites of different sizes [45]. The relationship between the crystallite diameter and the relative number of B_5-type sites is shown in Fig. 7; the number of active sites is correlated, however, with the number of surface atoms (the Jacobsen data [45] were recalculated with the formula of Borodziński and Bonarowska [54]). For comparison, the particle size dependence of TOF, as determined in the present study for one of the systems (Ba–Ru/C), is also presented in Fig. 7.

As seen in Fig. 7, the relative number of B_5 sites and TOF show the same trend in the scale of extra fine particles only ($d < 1.5$–2.0 nm). For larger sizes ($d > 2$ nm), a discrepancy is observed: whereas the concentration of B_5 sites decreases with particle diameter, TOF increases slowly vs d; an increase in TOF is also characteristic for the other promoted systems (Cs–Ru/C, Ba–Cs–Ru/C; see Fig. 6). One might suggest, therefore, that sites different from those of B_5 are engaged in the NH_3 synthesis reaction on ruthenium. According to the general considerations of Poltorak and Boronin [64], the specific activity (TOF) increases with increasing particle size (this is our case) when the metal

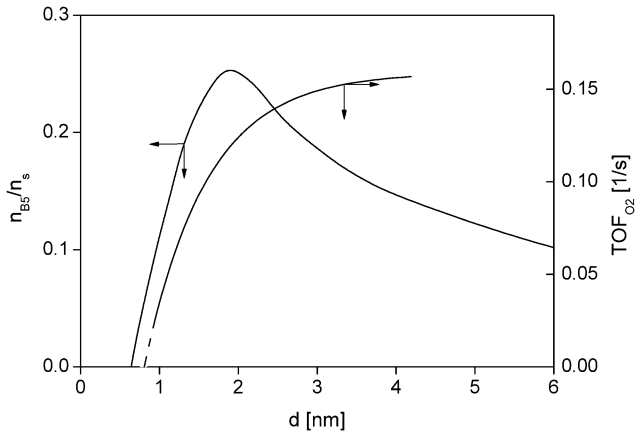

Fig. 7. Number of B_5-type sites (n_{B_5}) referred to the total number of surface atoms (n_S) and TOF of NH_3 synthesis for Ba–Ru/C vs particle diameter; trace n_{B_5}/n_S was determined using the data presented in [45].

atoms at the faces of the crystallites show a greater activity than those at the edges. However, such an interpretation does not find support in the literature. Single-crystal studies of Dahl et al. show [50] that the rate of nitrogen adsorption is dominated by steps; Ru atoms on terraces are almost inactive.

In a discussion of the discrepancy between the kinetic data (TOF) and results of predictions based on the theoretical approach (B_5 sites) at the scale of large particles (see Fig. 7), attention should be paid to the limitations of the assumptions used for determining the B_5 trace. That is, the calculations presented in [45] (see Fig. 7) are based on the assumption that the metal particles form perfect crystallites, that is, the shape and morphology of the crystallites remain unchanged with increasing diameter. This may not be true. Recent studies of model Ru/graphite systems demonstrate [65] that at low metal surface concentration (2 at%), the particles (~ 2 nm) have a round shape, and at high Ru surface concentration (> 10 at%), Ru forms flat particles; the latter are significantly more active in nitrogen desorption. It cannot be excluded, therefore, that the morphology of larger crystallites (3–4 nm) in unpromoted catalysts with high Ru loading is more advantageous (more B_5 sites are exposed) than that of the smaller crystallites. The optimal crystallite size, corresponding to the maximum B_5 site concentration on the Ru surface, would then be shifted to higher (d) values, possibly higher than 4 nm. We suggest, however, that the trends in TOF illustrated in Fig. 6 are determined by the presence of the promoters in the systems rather than by the relative number of B_5 sites in the unpromoted Ru/C precursors. Should the promoters be located at the faces of the ruthenium crystallites, the nearby metal atoms would be promoted and a systematic increase in the surface-based reaction rate (TOF) with the particle size would result. Further studies of specimens of low dispersion ($d > 4$ nm) are necessary to distinguish between the two options presented above.

The effect of co-promotion (synergy) is a separate question. To determine why doubly doped catalysts (see Fig. 6)

are more active than singly doped systems, the promoting mechanism (mechanisms) of caesium and barium should be considered. It is commonly believed that the main role of the alkali (K, Cs) is to lower the barrier for N_2 adsorption via electronic interaction of the promoter with the active metal [66–69]. Barium is supposed to act either as an electronic promoter [15,28,47,48], like alkali, or as a structural agent [18,36,37] that modifies the Ru surface morphology, thus increasing the number of highly active sites, possibly of the B_5 type. Recent microkinetic modelling performed by Siporin and Davis [70] for the NH_3 synthesis reaction proceeding on differently doped Ru/MgO catalysts shows, however, that the role of the promoters is more complex. Although the Cs promotion of Ru lowered the activation barrier for N_2 dissociation, the enthalpy of dihydrogen adsorption and, consequently, the H atom surface coverage increased slightly, resulting in a small but noticeable (a factor of 2) decrease in the relative number of free sites, that is, those accessible for N_2 adsorption [70]. Thus, the overall effect of caesium is a compromise between lowering the activation barrier for N_2 dissociation and increasing the competitive adsorption of H_2 [70]. In contrast to caesium, barium was found to lower the heat of H_2 adsorption, and the effect was rather strong [70]. Because of the shift in the equilibrium from adsorbed to gas-phase hydrogen, the number of free sites increased for Ba–Ru/MgO by a factor of 5 [70] compared with unpromoted Ru/MgO.

A strong decrease in the heat of H_2 adsorption upon promotion with barium seems to be a consequence of the ruthenium surface reconstruction rather than of electronic interaction between Ba and Ru. Support for this comes from the literature. Single-crystal studies of ruthenium have revealed that the activation energy of hydrogen desorption (E_{des}) and, consequently, the heat of H_2 adsorption (adsorption is a nonactivated process) are very sensitive to the metal surface structure. Jacobi [71] has shown that H_2 is adsorbed on the very open $(11\bar{2}1)$ plane in three different states ($E_{\mathrm{des}} = 20$, 31, and 50 kJ/mol, respectively [40]). Christmann and Muschiol [72] found the adsorption energies for the Ru $(10\bar{1}0)$ surface to vary between 56 and 80 kJ/mol. In the case of Ru (0001), E_{des} changes from about 80 to about 125 kJ/mol, depending on the preliminary coverage with H atoms. Variations in the heat of hydrogen adsorption to a metal surface structure were also reported for iron [73] and platinum [74].

Hence, the effect of synergy (Ba–Cs–Ru/C) should be ascribed to a different role of the promoters: whereas the alkali (Cs, K) acts essentially as an electronic promoter, barium influences mainly the surface morphology; electronic interactions are less important. The reconstructed surfaces in Ba–Ru/C (Ba–Cs–Ru/C) might expose new active sites (e.g., B_5), as suggested previously [18,36,37], but they would first of all be more resistant to poisoning by hydrogen under ammonia synthesis conditions, thus making more free sites available for nitrogen dissociation.

Acknowledgments

This work was done as part of Research Project 3 T09B 047 27, sponsored by the Polish Committee for Scientific Research. W. Raróg-Pilecka is grateful to the Foundation for Polish Science for financial support. Thanks are due to Dr. W.M.T.M. Reimerink at NORIT Nederland B.V. for supplying the carbon materials.

References

[1] R. Schloegl, Angew. Chem. Int. Ed. 42 (2003) 2004.
[2] K. Tamaru, in: J.R. Jennings (Ed.), Catalytic Ammonia Synthesis. Fundamentals and Practice, Plenum Press, New York, 1991, p. 1.
[3] J.A. Dumesic, H. Topsoe, M. Boudart, J. Catal. 37 (1975) 513.
[4] J.A. Dumesic, H. Topsoe, S. Khammouma, M. Boudart, J. Catal. 37 (1975) 503.
[5] D.R. Strongin, J. Carazza, S.R. Bare, G.A. Somorjai, J. Catal. 103 (1987) 213.
[6] D.R. Strongin, G.A. Somorjai, in: J.R. Jennings (Ed.), Catalytic Ammonia Synthesis. Fundamentals and Practice, Plenum Press, New York, 1991, p. 133.
[7] R.B. Strait, Nitrogen and Methanol 238 (1999) 37.
[8] R.B. Strait, S.A. Knez, in: International Conference Exhibition, Caracas, 28 February–2 March 1999.
[9] K. Aika, H. Hori, A. Ozaki, J. Catal. 27 (1972) 424.
[10] K. Aika, K. Shimazaki, Y. Hattori, A. Ohya, S. Ohshima, K. Shirota, A. Ozaki, J. Catal. 92 (1985) 296.
[11] S. Murata, K. Aika, J. Catal. 136 (1992) 118.
[12] S. Murata, K. Aika, J. Catal. 136 (1992) 110.
[13] K.S. Rama Rao, S. Khaja Masthan, P.S. Sai Prasad, P. Kanta Rao, Appl. Catal. A 73 (1991) L1.
[14] L. Forni, D. Molinari, I. Rossetti, N. Pernicone, Appl. Catal. A 185 (1999) 269.
[15] I. Rossetti, N. Pernicone, L. Forni, Appl. Catal. A 208 (2001) 271.
[16] I. Rossetti, N. Pernicone, L. Forni, Appl. Catal. A 248 (2003) 97.
[17] Z. Kowalczyk, J. Sentek, S. Jodzis, E. Mizera, J. Góralski, T. Paryjczak, R. Diduszko, Catal. Lett. 45 (1997) 65.
[18] W. Raróg, Z. Kowalczyk, J. Sentek, D. Składanowski, J. Zieliński, Catal. Lett. 68 (2000) 163.
[19] W. Raróg, I. Lenarcik, Z. Kowalczyk, J. Sentek, M. Krukowski, J. Zieliński, Pol. J. Chem. 74 (2000) 1473.
[20] Z. Kowalczyk, M. Krukowski, W. Raróg-Pilecka, D. Szmigiel, J. Zieliński, Appl. Catal. A: Gen. 248 (2003) 67.
[21] Ch. Liang, Z. Wei, Q. Xin, C. Li, Appl. Catal. A: Gen. 208 (2001) 193.
[22] X.L. Zhenh, S.J. Zhang, J. Xu, K.M. Wei, Carbon 40 (2002) 2597.
[23] Ch. Liang, Z. Li, J. Qiu, C. Li, J. Catal. 211 (2002) 278.
[24] H.S. Zeng, K. Inazu, K. Aika, Appl. Catal. A: Gen. 219 (2001) 235.
[25] Z. Zhong, K. Aika, J. Catal. 173 (1998) 535.
[26] Z. Zhong, K. Aika, Inorg. Chem. Acta 280 (1998) 183.
[27] S.M. Yunusov, E.S. Kalyuzhnaya, B.L. Moroz, S.N. Agafonova, V.A. Likholobov, V.B. Shur, J. Mol. Catal. A: Chem. 165 (2001) 141.
[28] S.E. Siporin, R.J. Davis, W. Raróg-Pilecka, D. Szmigiel, Z. Kowalczyk, Catal. Lett. 93 (2004) 61.
[29] Z. Li, Ch. Liang, Z. Feng, P. Ying, D. Wang, C. Li, J. Mol. Catal. A: Chem. 211 (2004) 103.
[30] S.E. Siporin, B.C. McClaine, S.L. Anderson, R.J. Davis, Catal. Lett. 81 (2002) 265.
[31] B.C. McClaine, S.E. Siporin, R.J. Davis, J. Phys. Chem. B 105 (2001) 7525.
[32] B.C. McClaine, T. Becue, C. Lock, R.J. Davis, J. Mol. Catal. A: Chem. 163 (2000) 105.
[33] B.C. McClaine, R.J. Davis, J. Catal. 211 (2002) 379.

[34] O. Hinrichsen, F. Rosowski, A. Hornung, M. Muhler, G. Ertl, J. Catal. 165 (1997) 33.
[35] F. Rosowski, A. Hornung, O. Hinrichsen, D. Herein, M. Muhler, G. Ertl, Appl. Catal. A 151 (1997) 443.
[36] H. Bielawa, O. Hinrichsen, A. Birkner, M. Muhler, Angew. Chemie Int. Ed. 40/6 (2001) 1061.
[37] D. Szmigiel, H. Bielawa, M. Kurtz, O. Hinrichsen, M. Muhler, W. Raróg, S. Jodzis, Z. Kowalczyk, L. Znak, J. Zieliński, J. Catal. 205 (2002) 205.
[38] B.C. McClaine, R.J. Davis, J. Catal. 210 (2002) 387.
[39] S.E. Siporin, R.J. Davis, J. Catal. 222 (2004) 315.
[40] C. Zupanc, A. Hornung, O. Hinrichsen, M. Muhler, J. Catal. 209 (2002) 501.
[41] K. Aika, A. Ohya, A. Ozaki, Y. Inoue, I. Yasumori, J. Catal. 92 (1985) 305.
[42] K. Aika, M. Kumasaka, T. Oma, O. Kato, H. Matsuda, N. Watanabe, K. Yamazaki, A. Ozaki, T. Onishi, Appl. Catal. A 28 (1986) 57.
[43] K. Aika, T. Takano, S. Murata, J. Catal. 136 (1992) 126.
[44] B. Fastrup, Catal. Lett. 48 (1997) 111.
[45] C.J.H. Jacobsen, S. Dahl, P.L. Hansen, E. Tornqvist, L. Jansen, H. Topsoe, D.V. Prip, P.B. Moenshaug, I. Chorkendorff, J. Mol. Catal. A: Chem. 163 (2000) 19.
[46] S. Dahl, J. Sehested, C.J.H. Jacobsen, E. Tornqvist, I. Chorkendorff, J. Catal. 192 (2000) 391.
[47] T.W. Hansen, P.L. Hansen, S. Dahl, C.J.H. Jacobsen, Catal. Lett. 84 (2002) 7.
[48] T.W. Hansen, J.B. Wagner, P.L. Hansen, S. Dahl, H. Topsoe, C.J.H. Jacobsen, Science 294 (2001) 1508.
[49] C.J.H. Jacobsen, J. Catal. 200 (2001) 1.
[50] S. Dahl, E. Tornqvist, I. Chorkendorff, J. Catal. 192 (2000) 381.
[51] D. Szmigiel, W. Raróg-Pilecka, E. Miśkiewicz, M. Gliński, Z. Kaszkur, Z. Kowalczyk, Appl. Catal. A 273 (2004) 105.
[52] Z. Kowalczyk, S. Jodzis, W. Raróg, J. Zieliński, J. Pielaszek, A. Presz, Appl. Catal. A 184 (1999) 95.
[53] Z. Kowalczyk, S. Jodzis, W. Raróg, J. Zieliński, J. Pielaszek, Appl. Catal. A 173 (1998) 153.
[54] A. Borodziński, M. Bonarowska, Langmuir 13 (1997) 5613.
[55] K.C. Taylor, J. Catal. 38 (1975) 229.
[56] N.E. Buyanova, A.P. Karnaukhov, N.G. Koroleva, I.D. Ratner, O.N. Černavska, Kinet. Katal. 13 (1972) 1533.
[57] Z. Kowalczyk, Catal. Lett. 37 (1996) 173.
[58] S. Błażewicz, A. Świątkowski, B.J. Trznadel, Carbon 37 (1999) 693.
[59] W. Raróg-Pilecka, D. Szmigiel, A. Komornicki, J. Zieliński, Z. Kowalczyk, Carbon 41 (2003) 579.
[60] M. Guraya, S. Sprenger, W. Raróg-Pilecka, D. Szmigiel, Z. Kowalczyk, M. Muhler, Appl. Surf. Sci. 238 (2004) 77.
[61] N.B. Shitova, M.N. Dobrynkin, A.S. Noskov, I.P. Prosvirin, V.I. Bukhtiyarov, D.I. Kochubei, P.G. Tsyrulnikov, D.A. Shlyapin, Kinet. Catal. 45 (2004) 414.
[62] R. von Hardeveld, A. von Montfoort, Surf. Sci. 4 (1966) 396.
[63] R. von Hardeveld, F. Hartog, Surf. Sci. 15 (1969) 189.
[64] O.M. Poltorak, V.S. Boronin, Russ. J. Phys. Chem. 40 (1966) 1436.
[65] Z. Song, T.H. Cai, J.C. Hanson, J.A. Rodriguez, J. Hrbek, J. Am. Chem. Soc. 126 (2004) 8576.
[66] G. Ertl, S.B. Lee, M. Weiss, Surf. Sci. 114 (1982) 527.
[67] G. Ertl, in: J.R. Jennings (Ed.), Catalytic Ammonia Synthesis: Fundamentals and Practice, Plenum Press, New York, 1991, p. 109.
[68] J.J. Mortensen, B. Hammer, J.K. Norskov, Phys. Rev. Lett. 80 (1998) 4333.
[69] J.K. Norskov, S. Holloway, N.D. Lang, Surf. Sci. 114 (1984) 65.
[70] S.E. Siporin, R.J. Davis, J. Catal. 225 (2004) 359.
[71] C.Y. Fan, K. Jacobi, Surf. Sci. 482–485 (2001) 21.
[72] K. Christmann, U. Muschiol, Z. Phys. Chem. 197 (1996) 155.
[73] F. Bozso, G. Ertl, M. Grunze, M. Weiss, Appl. Surf. Sci. 1 (1977) 103.
[74] S.R. Tennison, in: J.R. Jennings (Ed.), Catalytic Ammonia Synthesis: Fundamentals and Practice, Plenum Press, New York, 1991, p. 303.